Evaluation and Stability of PEDOT Polymer Electrodes for Li–O_2 Batteries

Citation: Amanchukwu, Chibueze V. et al. "Evaluation and Stability of PEDOT Polymer Electrodes for Li–O_2 Batteries." The Journal of Physical Chemistry Letters 7, 19 (October 2016): 3770–3775

As Published: http://dx.doi.org/10.1021/acs.jpclett.6b01986

Publisher: American Chemical Society (ACS)

Persistent URL: http://hdl.handle.net/1721.1/111173

Version: Author's final manuscript: final author's manuscript post peer review, without publisher's formatting or copy editing

Evaluation and Stability of PEDOT Polymer Electrodes for Li–O_2 Batteries

Chibueze V. Amanchukwu,[†,+] Magali Gauthier,[‡⊥] Thomas P. Batcho,[§] Chanez Symister,[¶] Yang Shao-Horn,[‡,§,‖] Julio M. D'Arcy,[*,¶] and Paula T. Hammond[*,†,+]

[†]Department of Chemical Engineering, Massachusetts Institute of Technology, Cambridge, MA 02139, USA.

[+]The David H. Koch Institute for Integrative Cancer Research, Massachusetts Institute of Technology, Cambridge, MA 02139, USA.

[‡]Electrochemical Energy Laboratory, Research Laboratory of Electronics, Massachusetts Institute of Technology, Cambridge, MA 02139, USA.

[§]Department of Materials Science and Engineering, Massachusetts Institute of Technology, Cambridge, MA 02139, USA

[‖]Department of Mechanical Engineering, Massachusetts Institute of Technology, Cambridge, MA 02139, USA

[¶]Department of Chemistry, Washington University in St. Louis, St. Louis, MO 63130, USA

[⊥]Present address: LEEL, NIMBE, CEA, CNRS, Université Paris-Saclay, CEA Saclay 91191 Gif-sur-Yvette, France

Corresponding authors:

PTH: hammond@mit.edu

JMD: jdarcy@wustl.edu

Abstract

Lithium-air (O_2) batteries have shown great promise because of their high gravimetric energy density – an order of magnitude greater than Li-ion – but challenges such as electrolyte and electrode instability have led to poor capacity retention and low cycle life. Positive electrodes such as carbon and inorganic metal oxides have been heavily explored, but the degradation of carbon and the limited surface area of the metal oxides limit their practical use. In this work, we study the electron-conducting polymer poly(3, 4-ethylendioxythiophene) (PEDOT) and show it can support oxygen reduction to form Li_2O_2 in a nonaqueous environment. We also propose a degradation mechanism, and show that the formation of sulfone functionalities on the PEDOT surface and cleavage of the polymer repeat unit impairs electron conductivity, and leads to poor cycling. Our findings are important in the search for new Li–O_2 electrodes, and the physical insights provided are significant and timely.

TOC Graphic

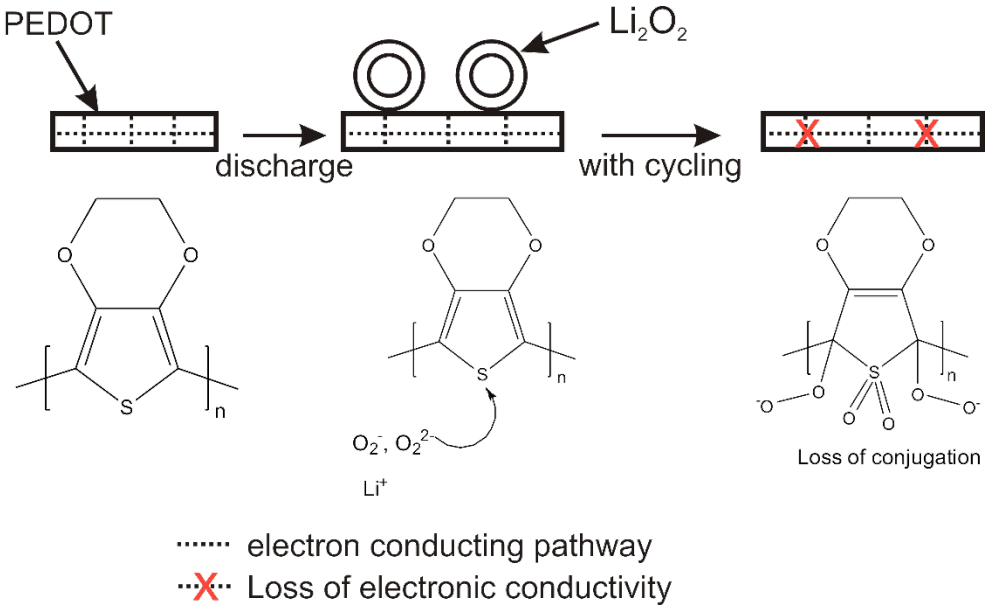

Lithium-air (O_2) batteries have shown promise as one of the energy-dense storage media of the future.[1-2] With a theoretical energy density (3500 Wh kg^{-1}_{Li2O2})[1] an order of magnitude greater than Li-ion, the quest for commercial Li–O_2 batteries has spurred great research interest. Despite their promise, Li–O_2 batteries have been plagued with numerous challenges such as the instability of the electrode and electrolyte, slow oxygen reduction and evolution kinetics, poor capacity retention with cycling and low cycle life.[2-4] Commonly used electrodes such as carbon have been shown to be unstable in the presence of lithium peroxide (Li_2O_2) – the desired discharge product – and superoxide intermediates during cycling.[5-6] Decomposition of carbon leads to insulating products such as lithium carbonate (Li_2CO_3) that are difficult to oxidize during charge and require high overpotentials.[5] Other cathodes such as nanoporous gold,[7] carbides[8] and inorganic metal oxides,[9] among others have been studied to replace carbon during Li–O_2 battery operation. Efficient cathodes for Li–O_2 need high surface area, good electronic conductivity, and low cost. Some electrode materials that may present these desirable properties include carbides and inorganic metal oxides; however, the limited surface area of these systems, and the cost of precious relatively inert metals such as gold limit their wide applicability in Li–O_2 batteries. Electron-conducting polymers are attractive as they have the desired electrode properties and are very easily processed into different cathode structures. Despite the numerous cathode types examined for Li–O_2, only few reports examining electron-conducting polymers for Li–O_2 cathodes exist.

Conducting polymers such as poly(3, 4-ethylendioxythiophene) (PEDOT),[10] poly(pyrrole),[11] and poly(aniline) have been widely explored as electrodes or electron-conducting binders for traditional Li-ion batteries. Typical binders such as poly(vinylidene fluoride) (PVDF) and polytetrafluoroethylene (PTFE) are not electronically conducting, and are used to bind composite

electrodes. Poly(pyrrole) served as both binder and electron conductor with a $LiMn_2O_4$ cathode,[11] and PEDOT has been used to eliminate the conventional carbon electron conducting matrix.[12] Furthermore, coating active electrode materials such as lithium cobalt oxide ($LiCoO_2$) and iron oxyfluoride (FeOF) with PEDOT can improve kinetics and limit the degradation and side reactions between the active material and the electrolyte solvent.[13-14] This strategy could be promising for Li–O_2 batteries where most organic insulating polymer binders such as PVDF have been shown to be unstable, as the ability of these conducting polymeric materials to transport electrons eliminates the need for further additives. [3, 15]

Cui *et al.*[16] studied tubular poly(pyrrole) as an electrode for Li–O_2 batteries, and show formation of lithium peroxide and charge/discharge over multiple cycles. Yoon *et al.*[17] recently reported the use of PEDOT:PSS (polystyrene sulfonate) to coat a graphene electrode and claim that PEDOT:PSS can suppress undesirable side reactions in the Li–O_2 cell and improve cycling performance. Nasybulin et al.[18] studied a Super P carbon/PEDOT composite as an electrode for Li–O_2 batteries, but the discharge performance and electrochemistry was dominated primarily by the carbon, and their use of a sulfone-containing salt like LiTFSI (lithium bis(trifluoromethane)sulfonimide) prevented a thorough understanding of PEDOT decomposition. The electron-conducting PEDOT was not evaluated as a stand-alone electrode despite its high electronic conductivity; serving primarily as a binder and contributing at most five percent of the obtained capacity.[18] In addition, these aforementioned studies did not explore the stability and mechanisms of degradation of the electron-conducting polymer upon cycling in Li–O_2 cells.

In this work, we examine the performance of a free-standing microstructured PEDOT electrode (with no carbon or binders present) in a Li–O_2 battery and show that it can support lithium

peroxide formation and Li–O_2 cycling. Our use of $LiClO_4$ as the electrolyte salt instead of LiTFSI allows for a clear understanding of the changes in the PEDOT structure. We show that the thiophene ring in PEDOT is susceptible to degradation that leads to sulfone formation, loss of conjugation in the polymer chain and diminished electronic conductivity that leads to poor cycling. Knowledge gained from this work can allow for greater understanding of the feasibility of using electron-conducting polymers as stand-alone Li–O_2 cathodes, and devising moieties that can avoid the observed degradation pathway of PEDOT. In addition, electron-conducting polymers could be used to coat cheap carbon particles to direct current and limit carbon reactivity and degradation in Li–O_2 cells.

The free-standing PEDOT films examined in this work were fabricated using an evaporative vapor-phase polymerization technique that generates the film directly from the substrate under conditions that yield fibrils of polymer film with nano- and microscale architectures.[19] Other fabrication methods such as in-situ deposition polymerization[20] or chemical vapor deposition (CVD)[21] can also yield PEDOT films with select architectures and high electronic conductivity. Furthermore, the examined PEDOT films lack the PSS polymer often used to acidically dope the polymer and aid its solubility in aqueous solutions and some organic emulsions. The use of a PEDOT-only electrode avoids addition of functionalities (such as PSS) that may complicate the understanding of PEDOT activity and the monitoring of changes induced by Li–O_2 reactions. The doped PEDOT films generated in this work have high electronic conductivity (130 S cm^{-1}), and have been fully characterized by D'Arcy et al.[19] The nanofibrillar architecture with high aspect ratio also makes it promising for Li–O_2 use because it will provide abundant nucleation sites for Li_2O_2 growth.

The ability of PEDOT to support crystalline Li_2O_2 formation after discharge without the addition of catalyst or other electron conducting media such as carbon was explored. Using lithium metal as the anode and a 0.1M $LiClO_4$ in DME electrolyte, PEDOT was able to support Li–O_2 discharge with a discharge plateau at 2.6 V reminiscent of the voltage at which oxygen reduction occurs with other Li–O_2 battery electrodes (Figure 1a).[22] Winter-Jensen et al.[23] have previously shown that the PEDOT surface is capable of supporting oxygen reduction, albeit in aqueous media. In conventional Li–ion batteries where PEDOT was evaluated as the electrode, low discharge capacities were observed because of poor intercalation of lithium ions. However, for Li–O_2 batteries, PEDOT does not need to intercalate lithium, but provide an electronically conducting surface that can support the diffusion and adsorption of O_2 and its subsequent reduction. X-ray diffraction (XRD) of the discharged electrode (Figure 1b) shows that Li_2O_2 is the primary discharge product, as evident from the (100) and (101) crystalline peaks.[22, 24] Furthermore, using scanning electron microscopy (SEM), one can observe the toroidal morphology associated with Li_2O_2 formation along the walls of the PEDOT electrode (Figure 1c).[22, 24]

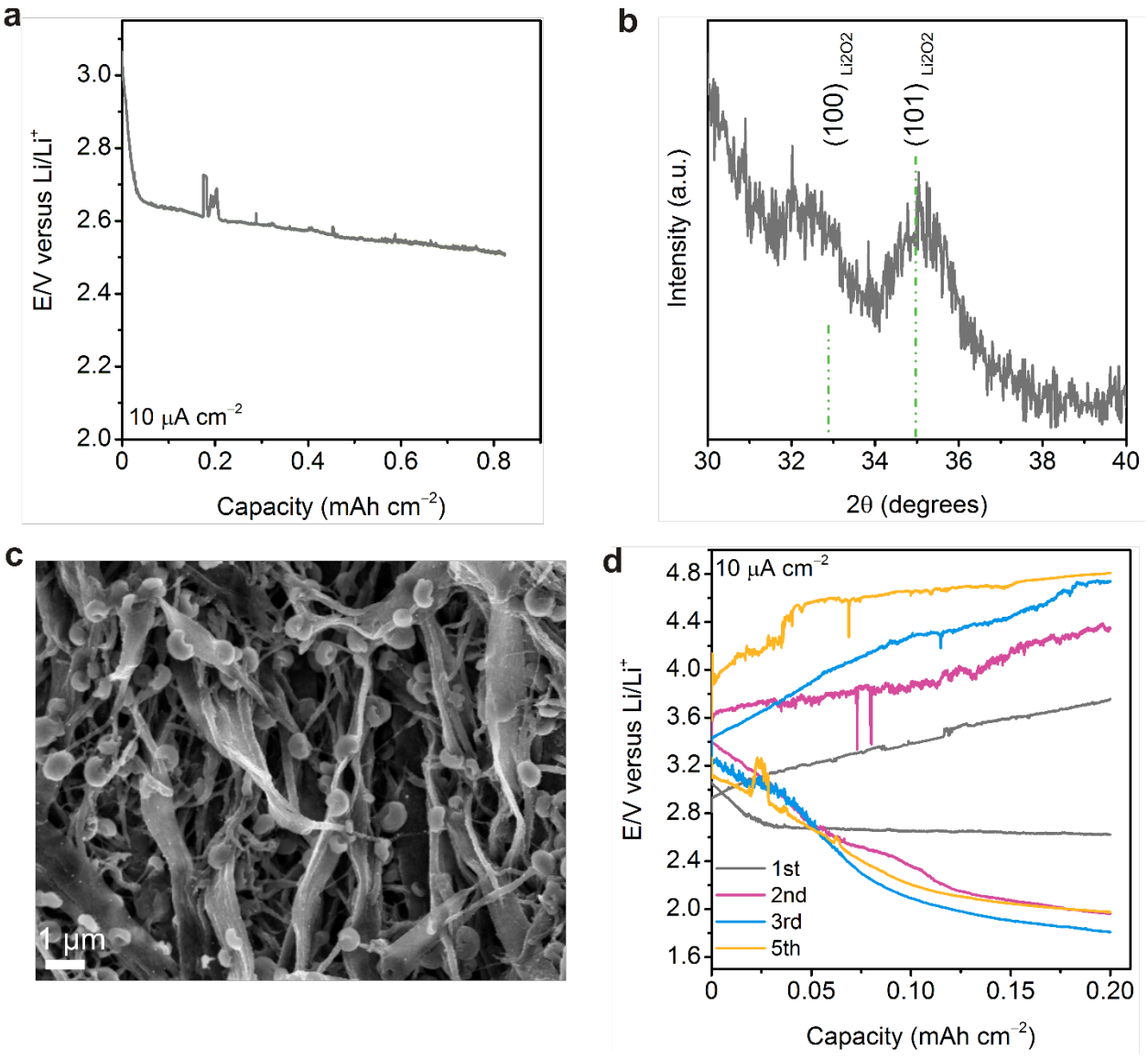

Figure 1. (a), Discharge curve of a Li–O_2 cell in O_2 at 10 μA cm^{-2} using a free-standing PEDOT electrode; (b), x-ray diffraction (XRD) and (c), Scanning electron microscopy (SEM) image after one discharge with a free-standing PEDOT electrode; (d) Five cycles at 10 μA cm^{-2} in O_2 using a free-standing PEDOT electrode. Figure 2a shows an SEM image of a pristine PEDOT electrode. Electrolyte: 0.1M $LiClO_4$ in DME.

Next, the PEDOT Li–O_2 cell was cycled five times using a capacity-limited regime at 0.2 mAh cm^{-2} (Figure 1d). The first discharge is similar to that observed in Figure 1 with the 2.6 V discharge voltage. The first charge is completed below 4 V, which is promising because typical carbon-based electrodes have higher charging potentials above 4 V and low energy efficiencies. Although the charging overpotential in the first cycle is low, subsequent cycling leads to higher discharge and charge overpotentials. By the fifth cycle, the discharge plateau is at 1.6 V and the charge culminates at 4.8 V.

SEM (Figure 2) was used to track the changes in the PEDOT architecture that may explain the poor cycling in Figure 1d. Figures 2a and b show a pristine and discharged electrode, respectively. As expected, toroids are abundant along the PEDOT network. After the first charge, Figure 2c shows disappearance of the Li_2O_2 toroids, revealing the original PEDOT structure. Therefore, PEDOT can support Li_2O_2 formation and oxidation in at least one cycle. By the fifth cycle, agglomerates are observed (Figure 2d) that may be due to an accumulation of decomposition from DME and PEDOT. DME is known to be unstable during Li–O_2 cycling,[6, 25-26] and prone to electrochemical oxidation above 4 V. The high charging voltages needed to complete charging on the PEDOT electrode may thus exacerbate the degradation of DME. Accumulation of insulating decomposition products such as Li_2CO_3 and acetates,[6] may then passivate the PEDOT surface, preventing oxygen reduction in subsequent cycles.

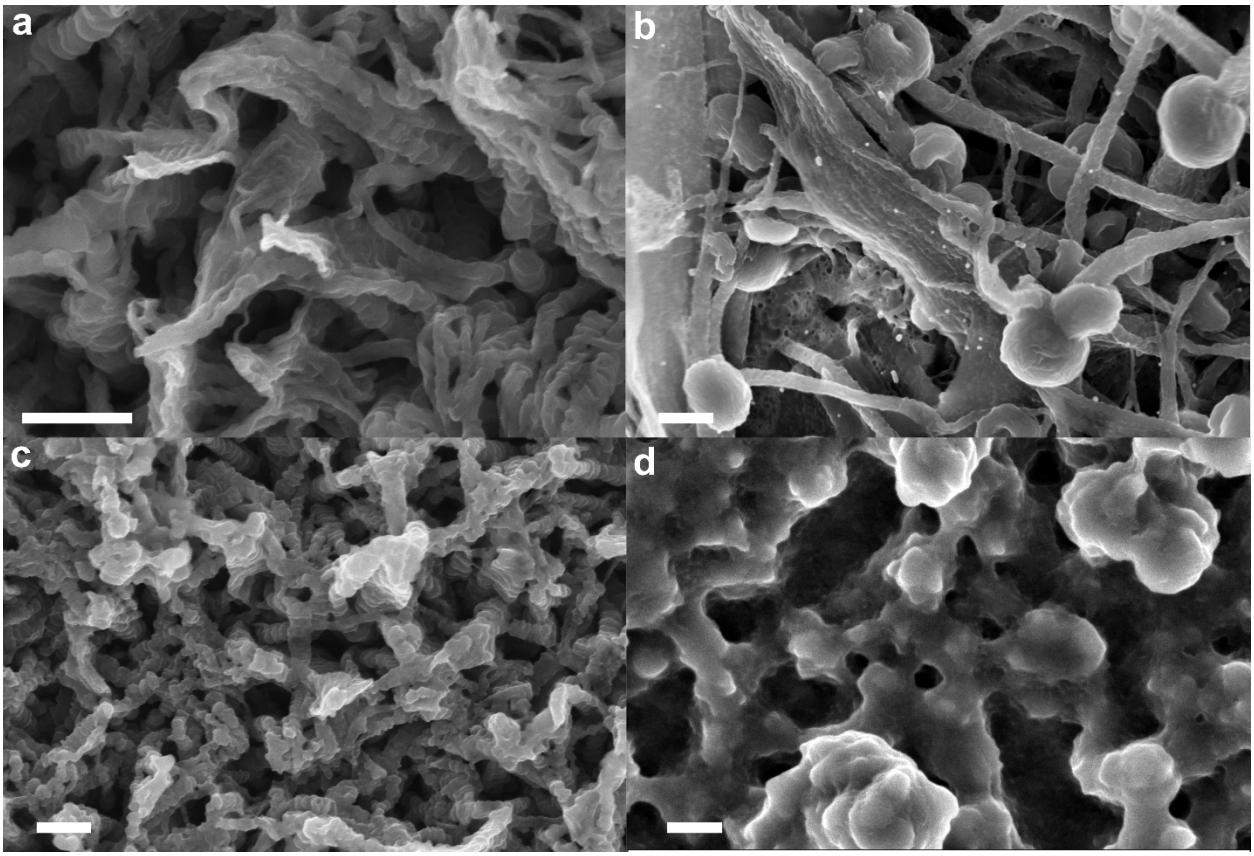

Figure 2. SEM images of pristine PEDOT electrode before discharge (a), after one discharge (b), one cycle (c), and five cycles (d). The free-standing PEDOT electrodes were discharged and charged at 10 μA cm^{-2} in O_2 in a 0.1M $LiClO_4$ in DME electrolyte. Scale bar = 500 nm.

To understand the stability of PEDOT, X-ray photoelectron spectroscopy (XPS) was used. Although electrochemical reduction to superoxide and consequently peroxide can occur on the PEDOT surface, these species are highly nucleophilic and can chemically attack PEDOT. Figure 3 shows C (1s), S (2p), and O (1s) spectra of the pristine PEDOT electrode and the electrode after 1 discharge, 1 cycle (ending on charge), and 5 cycles (ending on charge). The S (2p) spectra in Figure 3 show significant changes in the chemical environment of the S atom in PEDOT. As cycle number increases, the fraction of the higher binding energy peaks at ~169 ($S2p_{3/2}$) and

~170 eV ($S2p_{1/2}$) (relative to the original PEDOT peaks) increases. The shift to higher binding energy is due to sulfur atoms bound to a more electronegative atom like oxygen and those peaks have been attributed to sulfone.[27] Marciniak et al.[27] have shown that the PEDOT S atom can be attacked due to photooxidation and Verge et al.[28] have observed attack of the S atom in the presence of hydroxyl radicals.[28] Superoxide and peroxide anions are strong nucleophiles like hydroxyl, and may undergo similar reaction pathways with PEDOT (Supplementary Figure 1).

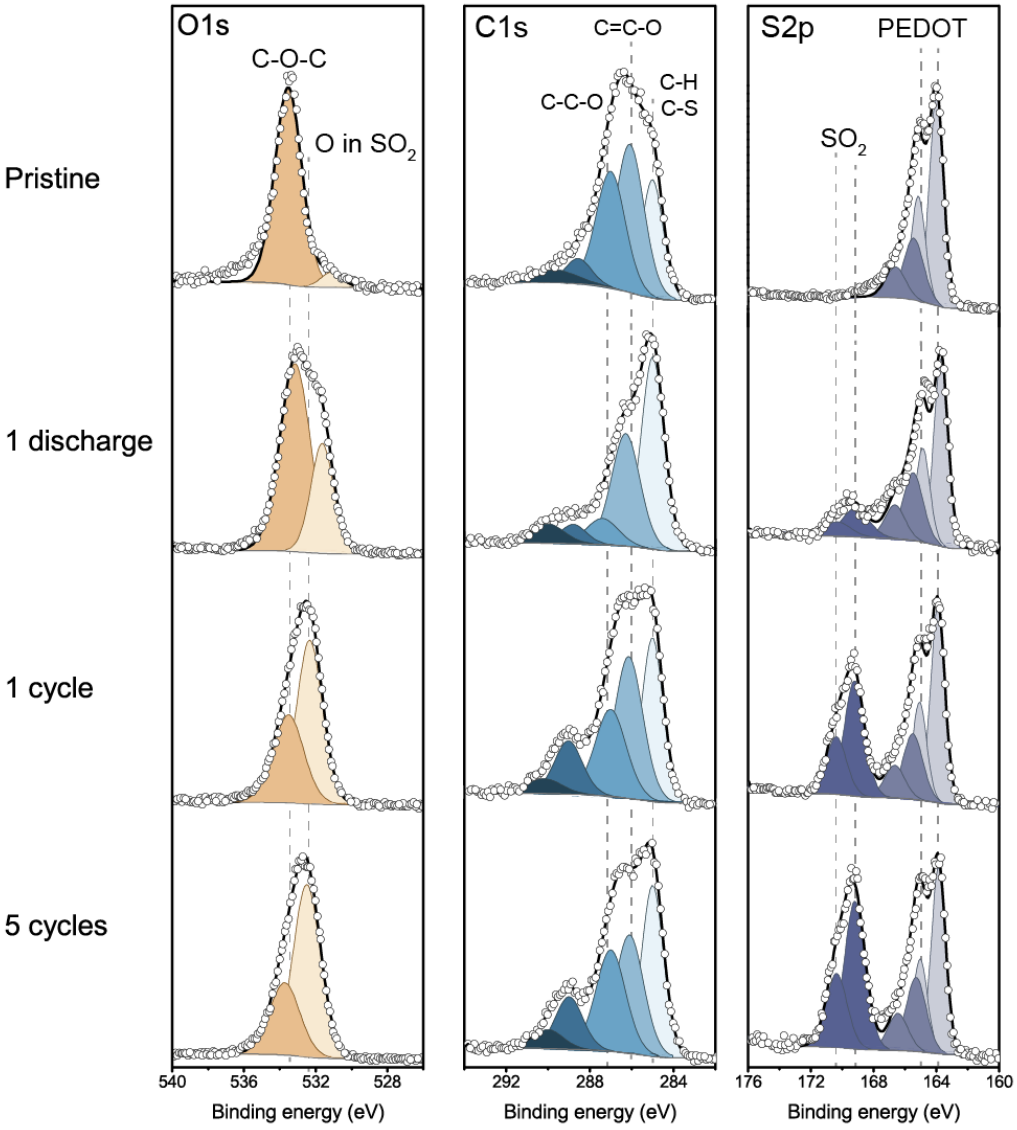

Figure 3. X-ray photoelectron spectroscopy (XPS) at the C (1s), O (1s) and S (2p) of a pristine PEDOT electrode, after one discharge, one cycle (ending on charge), and five cycles (ending on charge). The XPS spectra corresponds to the SEM images displayed in Figure 2. Details of the XPS deconvolution can be found in Supplementary Table 1.

The O (1s) spectra corroborate the observation in the S (2p) spectra. The fraction of the peak at 532 eV (compared to the total peak area) increases with cycling (Figure 4) and constitutes further evidence of the formation of a sulfone functionality. In addition, the O/S ratio provides a gauge of PEDOT oxidation because an increase in the ratio indicates oxygen external to PEDOT has been incorporated on the PEDOT surface or chemical structure. After the first discharge, Li_2O_2 is observed as expected at around 531 eV in the O (1s) spectra[29] in Figure 3, and may account for the high O/S ratio observed in Supplementary Table 2. However, with subsequent cycling that ends on charge, the O/S ratio is still higher than that observed in the pristine electrode and indicative of sulfone formation and oxygen-based DME decomposition species. The peak increase at 289 eV in the C (1s) spectra was postulated to be due to the formation of carbonyl/carboxyl groups on PEDOT or from DME oxidation or a shift due to the oxidized thiophene ring.[27] As Figure 4 shows, the fraction of oxidized products in the O (1s), C (1s), and S (2p) spectra increases with cycling.

In Supplementary Figure 1, we propose a mechanism for PEDOT degradation where oxygen reduction products from discharge and charge attack the partially positive S atom on the thiophene ring. A sulfoxide unit results and further addition to the S atom leads to formation of sulfone. Other sites on the PEDOT chemical structure can also be attacked as Verge et al.[28] show that OH radicals can oxidize the C–S–C bond. The formation of the sulfone functionality on the

PEDOT ring is an irreversible chemical change, and has been shown to lead to cleavage of the polymeric chain and a loss of conjugation.[27-28] Conjugation across the polymer backbone is responsible for electron conduction; therefore, the loss of conjugation decreases electronic conductivity, and may explain the inability of PEDOT to sustain further oxygen reduction after the first cycle (Figure 1d). [30-31]

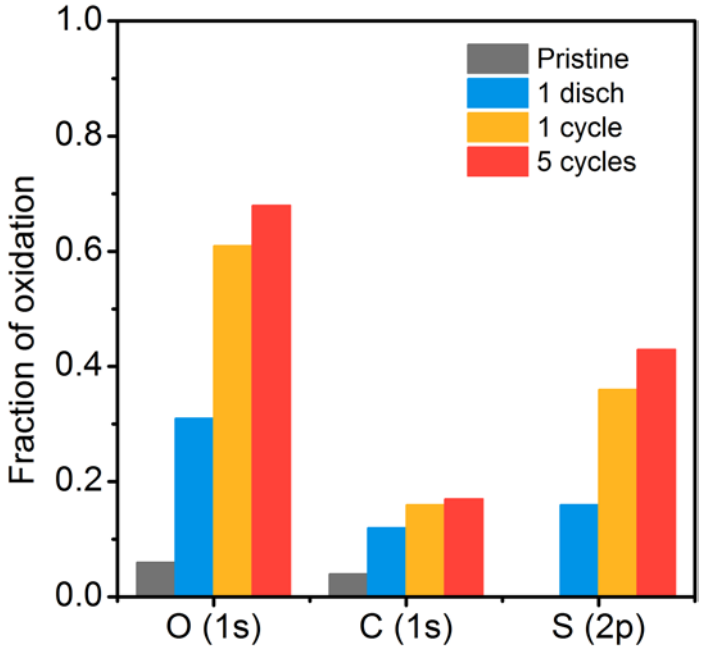

Figure 4. Fraction of oxidation products in the XPS O (1s), C (1s), and S (2p) spectra for the pristine PEDOT electrode, electrode after 1 discharge, 1 cycle (ending on charge), and 5 cycles (ending on charge). These fractions correspond to the XPS data in Figure 3. O (1s) fraction of oxidation = (532 eV peak area/ total peak area); C (1s) fraction of oxidation = (289 and 290 eV peak area/ total peak area); S (2p) fraction of oxidation = (169 and 170 eV peak area/ total peak area). The S (2p) spectra for the pristine has no peaks at 169 and 170 eV and has a “0” fraction.

In this work, we examined the performance of PEDOT as a stand-alone electrode in a Li–O_2 battery. We show that the conducting polymer PEDOT can initially support Li–O_2 discharge and charge with the formation and oxidation of Li_2O_2 respectively. However, after several discharges and charges, irreversible changes occur on PEDOT that lead to the oxidation of the thiophene ring and formation of sulfone, cleavage of segments of the polymer that lead to loss of conjugation and electronic conductivity; these changes result in poor cycling behavior. Therefore, the use of PEDOT is limited for binder or electrode use in Li–O_2 batteries. Knowledge gained from this work should galvanize the Li–O_2 community in developing new electronic conducting polymers that avoid the susceptibility of PEDOT S atom oxidation and loss of conjugation, and provide an alternative to the carbon and inorganic electrodes that have been heavily studied so far. These findings are important in the search for new Li–O_2 electrodes, of which electron-conducting polymers are an exciting prospect, and the physical insights related to PEDOT decomposition are significant and urgent.

Methods

Synthesis of PEDOT electrode: The free-standing PEDOT electrode was synthesized as previously reported in ref ([19]) using an evaporative vapor-phase polymerization procedure. In a chemical vapor deposition (CVD) chamber, a droplet of $FeCl_3$ aqueous oxidant solution is placed on a gold-coated substrate. An EDOT in chlorobenzene solution is also introduced into the chamber, and the temperature is ramped from 25 °C to 130 °C at 600 °C/h for polymerization to occur. The PEDOT is removed from the chamber, washed with water and methanol to remove excess oxidant, and stored in 6 M HCl. To prepare for Li–O_2 use, the electrodes were washed in copious amounts of milliQ water (18 mΩ cm) before washing with methanol. The electrodes were then vacuum-dried at 75 °C for at least two nights. The PEDOT electrode was soaked in excess 0.1 M $LiClO_4$ in DME electrolyte prior to cell fabrication.

Fabrication of Li–O_2 cell: Li–O_2 cells were fabricated in an Argon glovebox (MBRAUN, H_2O < 0.1 ppm, O_2 < 0.1 ppm). Using Li–O_2 cells fabricated in our laboratory,[32] 15 mm lithium metal (Alfa Aesar, 99.9% metals basis) was used as the anode, a 0.1 M $LiClO_4$ in DME electrolyte (BASF), two 18 mm Celgard C480 separators, and the PEDOT electrode. A stainless steel mesh (12.7 mm diameter) was used as the current collector. After fabrication, the Li–O_2 cell was moved without air exposure to another Argon glovebox (MBRAUN, H_2O < 0.1 ppm, O_2 < 1%) where it was filled with oxygen. The fabricated Li–O_2 cell was allowed to rest for 4 hours before any electrochemical tests were performed. After the electrochemical tests, the Li–O_2 cell was opened in an Argon glovebox without air exposure, and the PEDOT electrodes were stored.

Scanning Electron Microscope (SEM) characterization: Samples were imaged using a Zeiss Supra 55VP and a Zeiss Ultra 55 (Carl Zeiss AG, Germany). The working voltage was 5kV. Samples were mounted and sealed in an Argon glovebox in order to minimize the time (~< 5 sec) of exposure to ambient atmosphere during transfer into SEM.

X-ray diffraction characterization: Electrochemically-tested cells were opened in an Argon glovebox (MBRAUN, H_2O < 0.1 ppm, O_2 < 0.1 ppm) without air exposure. Samples were sealed in an airtight XRD sample holder (Anton Paar, Austria) to minimize air exposure before and during XRD measurement. A Rigaku Smartlab (Rigaku, Salem, NH) in the parallel beam configuration was used to collect the XRD spectra.

X-ray photoelectron spectroscopic (XPS) characterization: To avoid any exposure to air, samples were transferred from the glovebox to the XPS chamber using a sample transfer vessel (ULVAC-PHI, INC.) Spectra were collected with a PHI 5000 VersaProbe II (ULVAC-PHI, INC.) using a monochromatized Al K_α source, a pass energy of 23.5 eV and a charge neutralizer. All spectra were calibrated with the C1s photoemission peak of adventitious carbon at 285 eV. Photoemission lines were fitted using combined Gaussian-Lorentzian functions after subtraction of a Shirley-type background.

Associated Content

Supporting Information

Additional characterization and PEDOT degradation mechanism is provided. This material is available free of charge via the internet at http://pubs.acs.org.

Acknowledgments

This work was partially supported by the Samsung Advanced Institute of Technology (SAIT), and the facilities at the Koch Institute for Integrative Cancer Research. C.V.A is supported by the Department of Defense through the National Defense Science and Engineering Graduate (NDSEG) Fellowship, and the GEM Fellowship. T.B.P is supported by the Skoltech Electrochemical Center. SEM was performed at the Center for Nanoscale Systems (CNS) at Harvard University.

References

1. Bruce, P. G.; Freunberger, S. A.; Hardwick, L. J.; Tarascon, J.-M., Li-O2 and Li-S Batteries with High Energy Storage. *Nature Materials* **2011,** *11*, 19-29.

2. Kwabi, D.; Ortiz-Vitoriano, N.; Freunberger, S.; Chen, Y.; Imanishi, N.; Bruce, P.; Shao-Horn, Y., Materials Challenges in Rechargeable Lithium-Air Batteries. *MRS Bulletin* **2014,** *39*, 443-452.

3. Amanchukwu, C. V.; Harding, J. R.; Shao-Horn, Y.; Hammond, P. T., Understanding the Chemical Stability of Polymers for Lithium–Air Batteries. *Chemistry of Materials* **2015,** *27*, 550-561.

4. Kwabi, D. G.; Batcho, T. P.; Amanchukwu, C. V.; Ortiz-Vitoriano, N.; Hammond, P.; Thompson, C. V.; Shao-Horn, Y., Chemical Instability of Dimethyl Sulfoxide in Lithium–Air Batteries. *The Journal of Physical Chemistry Letters* **2014,** *5*, 2850-2856.

5. Ottakam Thotiyl, M. M.; Freunberger, S. A.; Peng, Z.; Bruce, P. G., The Carbon Electrode in Nonaqueous Li–O2 Cells. *Journal of the American Chemical Society* **2012,** *135*, 494-500.

6. McCloskey, B.; Speidel, A.; Scheffler, R.; Miller, D.; Viswanathan, V.; Hummelshøj, J.; Nørskov, J.; Luntz, A., Twin Problems of Interfacial Carbonate Formation in Nonaqueous Li–O2 Batteries. *The Journal of Physical Chemistry Letters* **2012,** *3*, 997-1001.

7. Peng, Z.; Freunberger, S. A.; Chen, Y.; Bruce, P. G., A Reversible and Higher-Rate Li-O2 Battery. *Science* **2012,** *337*, 563-566.

8. Thotiyl, M. M. O.; Freunberger, S. A.; Peng, Z.; Chen, Y.; Liu, Z.; Bruce, P. G., A Stable Cathode for the Aprotic Li–O2 Battery. *Nature Materials* **2013,** *12*, 1050-1056.

9. Kundu, D.; Black, R.; Berg, E. J.; Nazar, L. F., A Highly Active Nanostructured Metallic Oxide Cathode for Aprotic Li–O 2 Batteries. *Energy & Environmental Science* **2015,** *8*, 1292-1298.

10. Yao, Y.; Liu, N.; McDowell, M. T.; Pasta, M.; Cui, Y., Improving the Cycling Stability of Silicon Nanowire Anodes with Conducting Polymer Coatings. *Energy & Environmental Science* **2012,** *5*, 7927-7930.

11. Kuwabata, S.; Masui, S.; Yoneyama, H., Charge–Discharge Properties of Composites of Limn 2 O 4 and Polypyrrole as Positive Electrode Materials for 4 V Class of Rechargeable Li Batteries. *Electrochimica Acta* **1999,** *44*, 4593-4600.

12. Arbizzani, C.; Mastragostino, M.; Rossi, M., Preparation and Electrochemical Characterization of a Polymer Li 1.03 Mn 1.97 O 4/Pedot Composite Electrode. *Electrochemistry Communications* **2002,** *4*, 545-549.

13. Her, L.-J.; Hong, J.-L.; Chang, C.-C., Preparation and Electrochemical Characterizations of Poly (3, 4-Dioxyethylenethiophene)/Licoo 2 Composite Cathode in Lithium-Ion Battery. *Journal of Power Sources* **2006,** *157*, 457-463.

14. Fan, X.; Luo, C.; Lamb, J.; Zhu, Y.; Xu, K.; Wang, C., Pedot Encapsulated Feof Nanorod Cathodes for High Energy Lithium-Ion Batteries. *Nano Letters* **2015,** *15*, 7650-7656.

15. Black, R.; Oh, S. H.; Lee, J.-H.; Yim, T.; Adams, B.; Nazar, L. F., Screening for Superoxide Reactivity in Li-O2 Batteries: Effect on Li2o2/Lioh Crystallization. *Journal of the American Chemical Society* **2012,** *134*, 2902-2905.

16. Cui, Y.; Wen, Z.; Liang, X.; Lu, Y.; Jin, J.; Wu, M.; Wu, X., A Tubular Polypyrrole Based Air Electrode with Improved O 2 Diffusivity for Li–O 2 Batteries. *Energy & Environmental Science* **2012,** *5*, 7893-7897.

17. Yoon, D. H.; Yoon, S. H.; Ryu, K.-S.; Park, Y. J., Pedot: Pss as Multi-Functional Composite Material for Enhanced Li-Air-Battery Air Electrodes. *Scientific Reports* **2016,** *6*.

18. Nasybulin, E.; Xu, W.; Engelhard, M. H.; Li, X. S.; Gu, M.; Hu, D.; Zhang, J.-G., Electrocatalytic Properties of Poly (3, 4-Ethylenedioxythiophene)(Pedot) in Li-O 2 Battery. *Electrochemistry Communications* **2013,** *29*, 63-66.

19. D'Arcy, J. M.; El-Kady, M. F.; Khine, P. P.; Zhang, L.; Lee, S. H.; Davis, N. R.; Liu, D. S.; Yeung, M. T.; Kim, S. Y.; Turner, C. L., Vapor-Phase Polymerization of Nanofibrillar Poly (3, 4-Ethylenedioxythiophene) for Supercapacitors. *ACS Nano* **2014,** *8*, 1500-1510.

20. Hohnholz, D.; MacDiarmid, A. G.; Sarno, D. M.; Jones Jr, W. E., Uniform Thin Films of Poly-3, 4-Ethylenedioxythiophene (Pedot) Prepared by in-Situ Deposition. *Chemical Communications* **2001**, 2444-2445.

21. Lock, J. P.; Im, S. G.; Gleason, K. K., Oxidative Chemical Vapor Deposition of Electrically Conducting Poly (3, 4-Ethylenedioxythiophene) Films. *Macromolecules* **2006,** *39*, 5326-5329.

22. Lu, Y.-C.; Kwabi, D. G.; Yao, K. P.; Harding, J. R.; Zhou, J.; Zuin, L.; Shao-Horn, Y., The Discharge Rate Capability of Rechargeable Li–O2 Batteries. *Energy & Environmental Science* **2011,** *4*, 2999-3007.

23. Winther-Jensen, B.; Winther-Jensen, O.; Forsyth, M.; MacFarlane, D. R., High Rates of Oxygen Reduction over a Vapor Phase–Polymerized Pedot Electrode. *Science* **2008,** *321*, 671-674.

24. Mitchell, R. R.; Gallant, B. M.; Thompson, C. V.; Shao-Horn, Y., All-Carbon-Nanofiber Electrodes for High-Energy Rechargeable Li–O 2 Batteries. *Energy & Environmental Science* **2011,** *4*, 2952-2958.

25. Freunberger, S. A.; Chen, Y.; Drewett, N. E.; Hardwick, L. J.; Bardé, F.; Bruce, P. G., The Lithium–Oxygen Battery with Ether-Based Electrolytes. *Angewandte Chemie International Edition* **2011,** *50*, 8609-8613.

26. McCloskey, B.; Bethune, D.; Shelby, R.; Girishkumar, G.; Luntz, A., Solvents' Critical Role in Nonaqueous Lithium–Oxygen Battery Electrochemistry. *The Journal of Physical Chemistry Letters* **2011,** *2*, 1161-1166.

27. Marciniak, S.; Crispin, X.; Uvdal, K.; Trzcinski, M.; Birgerson, J.; Groenendaal, L.; Louwet, F.; Salaneck, W. R., Light Induced Damage in Poly (3, 4-Ethylenedioxythiophene) and Its Derivatives Studied by Photoelectron Spectroscopy. *Synthetic Metals* **2004,** *141*, 67-73.

28. Verge, P.; Vidal, F.; Aubert, P.-H.; Beouch, L.; Tran-Van, F.; Goubard, F.; Teyssié, D.; Chevrot, C., Thermal Ageing of Poly (Ethylene Oxide)/Poly (3, 4-Ethylenedioxythiophene) Semi-Ipns. *European Polymer Journal* **2008,** *44*, 3864-3870.

29. Lu, Y.-C.; Crumlin, E. J.; Veith, G. M.; Harding, J. R.; Mutoro, E.; Baggetto, L.; Dudney, N. J.; Liu, Z.; Shao-Horn, Y., In Situ Ambient Pressure X-Ray Photoelectron Spectroscopy Studies of Lithium-Oxygen Redox Reactions. *Scientific Reports* **2012,** *2*.

30. Dietz, K.; Beck, F., Positive Polyacetylene Electrodes in Aqueous Electrolytes. *Journal of Applied Electrochemistry* **1985,** *15*, 159-166.

31. Vork, F.; Schuermans, B.; Barendrecht, E., Influence of Inserted Anions on the Properties of Polypyrrole. *Electrochimica Acta* **1990,** *35*, 567-575.

32. Harding, J. R.; Amanchukwu, C. V.; Hammond, P. T.; Shao-Horn, Y., Instability of Poly (Ethylene Oxide) Upon Oxidation in Lithium–Air Batteries. *The Journal of Physical Chemistry C* **2015,** *119*, 6947-6955.

Evaluation and Stability of PEDOT Polymer Electrodes for Li–O_2 Batteries

Chibueze V. Amanchukwu,[†,+] Magali Gauthier,[‡⊥] Thomas P. Batcho,[§] Chanez Symister,[¶] Yang Shao-Horn,[‡,§,‖] Julio M. D'Arcy,[*,¶] and Paula T. Hammond[*,†,+]

[†]Department of Chemical Engineering, Massachusetts Institute of Technology, Cambridge, MA 02139, USA.

[+]The David H. Koch Institute for Integrative Cancer Research, Massachusetts Institute of Technology, Cambridge, MA 02139, USA.

[‡]Electrochemical Energy Laboratory, Research Laboratory of Electronics, Massachusetts Institute of Technology, Cambridge, MA 02139, USA.

[§]Department of Materials Science and Engineering, Massachusetts Institute of Technology, Cambridge, MA 02139, USA

[‖]Department of Mechanical Engineering, Massachusetts Institute of Technology, Cambridge, MA 02139, USA

[¶]Department of Chemistry, Washington University in St. Louis, St. Louis, MO 63130, USA

[⊥]Present address: LEEL, NIMBE, CEA, CNRS, Université Paris-Saclay, CEA Saclay 91191 Gif-sur-Yvette, France

Corresponding authors:

PTH: hammond@mit.edu

JMD: jdarcy@wustl.edu

Supplementary Table 1. O (1s), C (1s), and S (2p) X-ray photoelectron spectroscopy (XPS) values obtained from pristine PEDOT films, after 1st discharge, after 1 cycle (ending on charge), and after 5 cycles (ending on charge).

O1s

	Position (eV)	FWHM	Area/(RSF*T*MFP)
Pristine	533.53	1.775	131.4
	531.11	1.368	7.9
1st discharge	533.15	2	218.2
	531.63	1.5	95.8
1st charge	533.51	2	102.1
	532.34	1.691	160.7
5th charge	533.73	2	84.0
	532.49	1.813	181.5

C1s

	Position (eV)	FWHM	Area/(RSF*T*MFP)
Pristine	285	1.2	377.0
	286.09	1.6	630.7
	287	1.641	508.2
	288.55	1.456	30.9
	289.72	2.48	27.2
1st discharge	285	1.29	608.9
	286.29	1.6	442.3
	287.4	1.8	115.1
	288.8	1.466	69.7
	290	1.849	87.4
1st charge	285	1.2	378.2
	286.14	1.6	437.1
	287	1.752	293.1
	289.02	1.573	161.5
	290.17	2	56.6
5th charge	285	1.235	392.
	286.11	1.597	352.1
	287	1.669	315.0
	288.99	1.538	150.0
	290	1.704	59.7

S2p

	Name	Position (eV)	FWHM	Area/(RSF*T*MFP)
Pristine	S 2p3/2	163.99	1.063	46.1
	S 2p1/2	165.15	1.063	23.0
	S 2p3/2 2	165.44	1.5	19.2
	S 2p1/2 2	166.6	1.5	9.6
1st discharge	S 2p3/2	163.7	1.066	21.1
	S 2p1/2	164.86	1.066	10.5
	S 2p3/2 2	165.48	1.5	10.7
	S 2p1/2 2	166.64	1.5	5.3
	S 2p	169.15	2	6.0
	S 2p	170.31	2	3.0
1st charge	S 2p3/2	163.91	1.066	22.0
	S 2p1/2	165.07	1.066	11.0
	S 2p3/2 2	165.5	1.5	10.3
	S 2p1/2 2	166.66	1.5	5.2
	S 2p	169.22	1.523	18.4
	S 2p	170.38	1.523	9.2
5th charge	S 2p3/2	163.86	1.072	18.5
	S 2p1/2	165.02	1.072	9.2
	S 2p3/2 2	165.29	1.5	10.3
	S 2p1/2 2	166.45	1.5	5.1
	S 2p	169.19	1.574	21.5
	S 2p	170.35	1.574	10.7

Supplementary Table 2. This table was used to make Figure 4 in the main manuscript. The values were obtained using the area values in Supplementary Table 1.

	C (1s)	O (1s)	S (2p)	O/S ratio
Pristine	0.04	0.06	0	1.4
1st discharge	0.12	0.31	0.16	5.5
1st charge	0.16	0.61	0.36	3.4
5th charge	0.17	0.68	0.43	3.5

The ratios in the table were obtained as follows: C (1s) = (Area at 288.9 + Area at 290 eV)/ total C (1s) area; O (1s) = Area at lower energy level (531 or 532 eV)/ Total area; S (2p) = (Area at 169 + area at 170 eV) / total S (2p) area; O/S ratio = total O (1s) area / total S (2p) area.

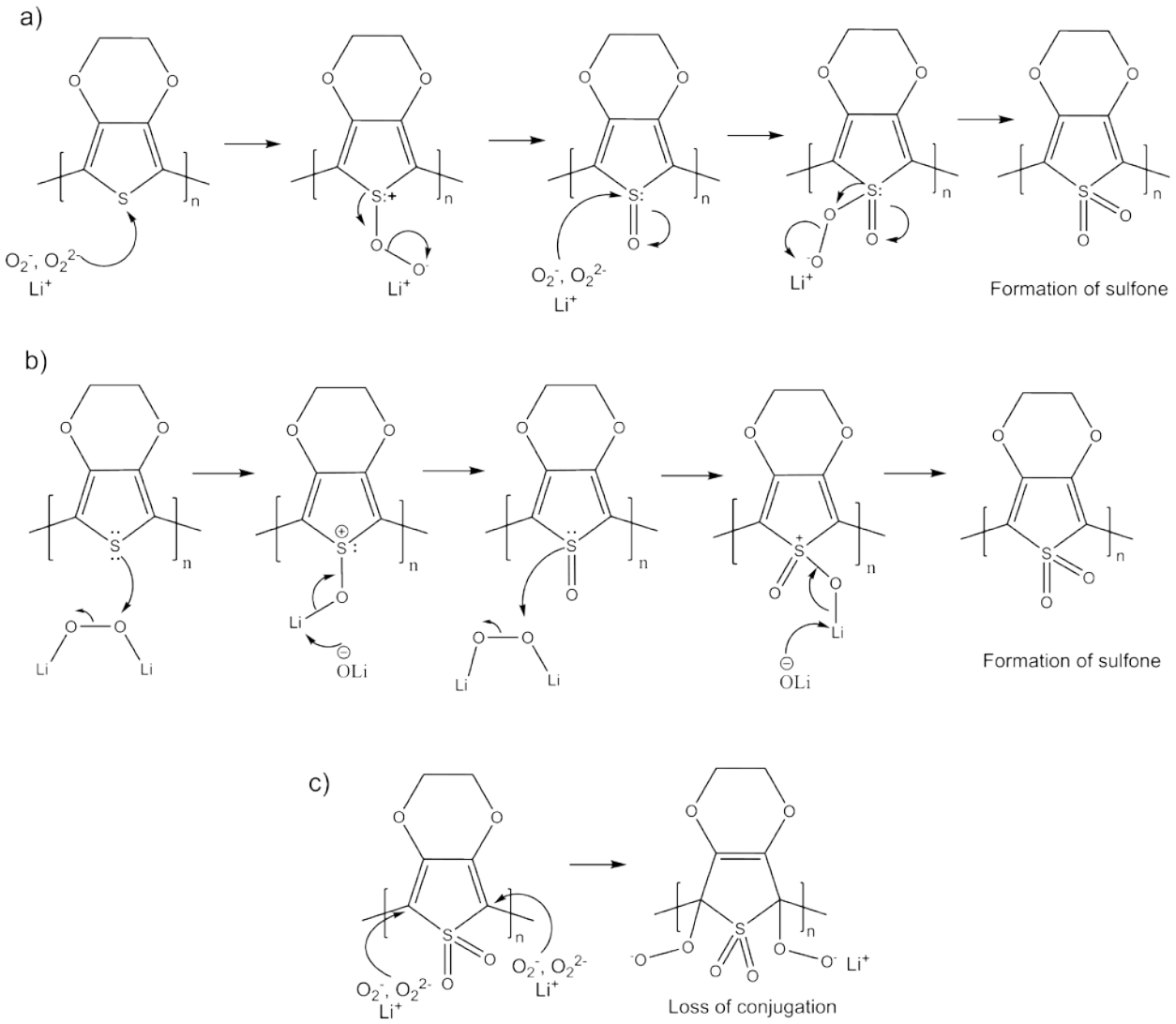

Supplementary Figure 1 | Proposed mechanism for the reaction of reduced oxygen species such as peroxide and superoxide with PEDOT where superoxide/peroxide attacks the S atom (**a**) or when the S atom of PEDOT attacks Li_2O_2 (**b**) that leads to formation of sulfone functionality. (**c**) Further reaction of the sulfone that leads to loss of conjugation and diminished electron conductivity. The counter-ion for all the negatively charged species in the schematic is lithium.